An original recycling method for Li-ion batteries through large scale production of Metal Organic Frameworks

Marine Cognet, Julie Condomines, Julien Cambedouzou, Srinivasan Madhavi, Michaël Carboni, Daniel Meyer

Journal of Hazardous Materials 385 (2020) 121603

Contents lists available at ScienceDirect

Journal of Hazardous Materials

journal homepage: www.elsevier.com/locate/jhazmat

An original recycling method for Li-ion batteries through large scale production of Metal Organic Frameworks

Marine Cognet[a], Julie Condomines[a], Julien Cambedouzou[a], Srinivasan Madhavi[b,c], Michaël Carboni[a,*], Daniel Meyer[a]

[a] ICSM (UMR 5257), CEA, CNRS, ENSCM, Univ Montpellier, Bagnols-sur-Cèze 30207, France
[b] School of Materials Science and Engineering, Nanyang Technological University, 50 Nanyang Avenue, Singapore
[c] Energy Research Institute @ NTU, Nanyang Technological University, 50 Nanyang Drive, Singapore, Singapore

GRAPHICAL ABSTRACT

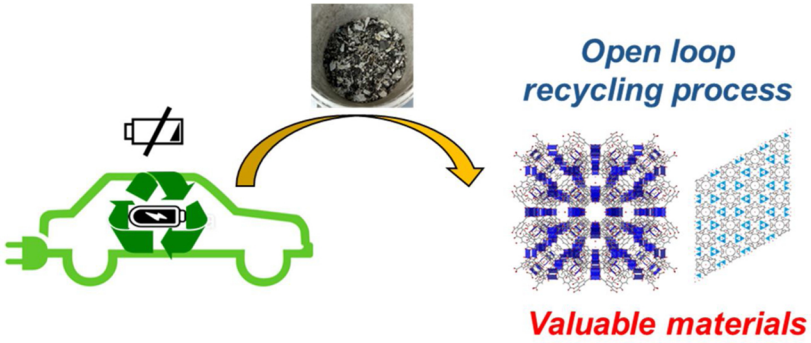

ARTICLE INFO

Editor: Dr. Danmeng Shuai

Keywords:
Recycling
Lithium-ion battery
Metal Organic Frameworks
Selective precipitation
Hydrometallurgy process

ABSTRACT

A concept is proposed for the recycling of Li-ion batteries with an open-loop method that allows to reduce the volume of wastes and simultaneously to produce valuable materials in large amounts (Metal-Organic Frameworks, MOFs). After dissolution of Nickel, Manganese, Cobalt (NMC) batteries in acidic solution (HCl, HNO_3 or H_2SO_4/H_2O_2), addition of organic moieties and a heat treatment, different MOFs are obtained. Solutions after precipitation are analyzed by inductively coupled plasma and materials are characterized by powder X-Ray diffraction, N_2 adsorption, thermogravimetric analysis and Scanning electron microscope. With the use of Benzene-Tri-Carboxylic Acid as ligand, it has been possible to form selectively a MOF, based on Al metallic nodes, called MIL-96 in the literature, and known for its interesting properties in gas storage applications. The supernatant is then used again to precipitate other metals as MOFs after addition of a second batch of ligands. These two other MOFs are based on Cu (known as HKUST-1 in the literature) or Ni-Mn (with a new crystalline structure) depending of conditions. This method shows promising results at the lab scale (15 g of wastes can be converted in 10 g of MOFs), and opens interesting perspectives for the scaled-up production of MOFs.

* Corresponding author at: ICSM (UMR 5257), CEA, CNRS, ENSCM, Univ Montpellier, Bagnols-sur-Cèze 30207, France.
E-mail address: michael.carboni@cea.fr (M. Carboni).

https://doi.org/10.1016/j.jhazmat.2019.121603
Received 6 June 2019; Received in revised form 22 October 2019; Accepted 2 November 2019
Available online 05 November 2019

1. Introduction

Batteries have been extensively developed as mobile energy sources (mobile, cars…) or for energy storage, which is crucial for the development of renewable energy technologies (Whittingham, 2012). There are currently many types of batteries with different advantages and limitations depending of the desired application. One of them, the Li-Ion battery (LiB), has been extensively developed since early 90s due to its rechargeable nature, high energy density and relative safety (Tarascon and Armand, 2001). LiBs are composed of a cathode, an anode, an electrolyte and a separator. Where the anode is a copper plate coated with a compound of graphite, the cathode is generally composed of metal oxides (LCO and NMC) (Rozier and Tarascon, 2015) or metal phosphates (LFP) (Dimesso et al., 2012) deposited on an aluminum plate. The LCO and NMC batteries, composed respectively of Co and Ni, Mn, Co oxides, have been widely produced until 2010 whereas the LFP production has drastically increased over the past 10 years and these 3 types of batteries now represent 90% of the overall production of the market (Pillot, 2017). Even if the $LiNi_{0.33}Mn_{0.33}Co_{0.33}O_2$ (NMC333) has been the common form of NMC (Cheng et al., 2017), different metal ratios have been introduced in the material and the trend is now to increase the energy density in place of the thermal stability and capacity retention by increasing the quantity of Ni in the composition (like NMC 622 or NMC 811) (Susai et al., 2018).

The worldwide spent LiBs are estimated to hit 2 million metric tons per year in 2030 due to the popularity of electronic cars (Jacoby, 2019). Even if batteries are valuable and recyclable (Ciez and Whitacre, 2019) due to technical or economic factors, less than 5% are collected and recycled today (Anon., 2019) even if some laws, as the Directive EU 2006/66/CE in Europe, state that 50% of LIBs in weight should be recycled. The sustainable recycling of LiBs is crucial for the development of this technology for the next decades (Liu et al., 2019; Zhang et al., 2018). Moreover metal resources needed for their synthesis are limited (Vikström et al., 2013) and the fast-growing concept of urban mine is essential due to the short economic life of electrical and electronic equipment's (Anon, 2013). However, the variability in the batteries' composition and the types of batteries increase the difficulty to develop an efficient recycling process (Grey and Tarascon, 2017). Generally, to recover materials from waste, a physical pretreatment is usually applied to obtain different streams of waste that are then treated by chemical methods (pyrometallurgy and hydrometallurgy mainly) (Xu et al., 2008). Even if the development of the hydrometallurgy treatment makes it a promising approach for the recycling of batteries (milder conditions and higher recovery of metals) (Chagnes and Pospiech, 2013), other non-conventional methods should be explored to increase the economic interest for battery recycling (Barik et al., 2016). The actual strategy is to develop a full close-loop recycling process (Gao et al., 2017) of every part of the battery (Rothermel et al., 2016), despite a low economic interest since raw materials remain cheap. In this way, an original route would be to generate high valuable products from a waste stream, creating an economical open-loop battery model for some metals instead of developing methods to isolate each component of the battery and to close the loop by re-manufacturing new batteries.

As valuable materials, Metal-Organic Frameworks (MOFs) are hybrid materials obtained by the assembling of organic moieties around metals or clusters (Cui et al., 2016). Due to their high crystallinity, porosity and versatile structure, they have been used in many applications such as gas storage or gas separation (Li et al., 2009). We have recently demonstrated their interest to mimic LFP electrodes in coin cells, where batteries have revealed high capacity and good cyclability over charge-discharge cycles (Cognet et al., 2017). The main difficulty of the use of such materials at an industrial level is the possibility to obtain them at large scale with a good purity by a process meeting industrial requirements (Silva et al., 2015). Generally, they are synthesized at the mg scale with large amount of toxic solvent (e.g. DMF). However, some techniques have recently been proposed to scale-up the process to the order of kg with the recycling of the solvent (Muller et al., 2006). The solvothermal strategy is probably the most suitable for a kt/year scale production, but other methods have been developed to solve inherent difficulties of such technique (e.g. high pressure and temperature or large quantity of solvent) (Yilmaz et al., 2012). The use of metallic oxides or sulfates are usually used for a solvothermal synthesis, as well as the use of carboxylic acids ligands as organic linkers. Among these techniques, a continuous electrochemical method has been developed to generate a Cu-MOF (HKUST-1) (Chui, 1999) with 1,3,5-benzenetricarboxylic acid and a copper cathode in solution (Muller et al., 2019). The obtained material has revealed some interesting properties for gas methane (Peng et al., 2013) and hydrogen (Xiao et al., 2007) storage or water adsorption (Liu et al., 2010). This method is used by BASF for the commercialization HKUST-1 under denomination "Basolite C300", but so far no other MOF has been reported using this method. Replacing nitrate or chloride salt by sulfate in aqueous solution at ambient pressure and low temperature (60 °C) results in an Al-MOF, also proposed by BASF (Basolite M050). Another interesting strategy is the use of mecanochemistry techniques (James et al., 2012) as developed and patented by MOF Technologies™. Even if the crystallinity and purity of such MOFs are not as good as those obtained by solvothermal synthesis (Ali-Moussa et al., 2017), it is still a credible technology that uses a small amount of solvent and reduces the time-scale preparation. However, this method faces some challenges (energy cost, crystallinity and purity of the materials …), and others approaches should be developed for the large-scale production of MOFs, of the same order than synthetic zeolites annual production (around 1.8 million metric tons) (Yilmaz et al., 2012).

We propose in this work to combine the recycling of batteries with a hydrothermal method leading to the large scale formation of MOFs. When NMC batteries are dissolved in acidic conditions, metals (Cu, Al, Ni, Mn, Co …) are released in solution. The addition of organic moieties in solution followed by a heat treatment has allowed us to obtain 3 different MOFs; two are known in the literature as MIL-96 and HKUST-1 and another one exhibits a new crystalline structure. These MOFs have potential applications as gas storage materials or also as new electrode materials for Li-Ion batteries. The synthesis of valuable materials from waste is an interesting strategy to reduce the volume of the battery wastes and to make the recycling process of LiBs economically viable by an open-loop cycle. This proof of concept can be extended for the recycling of other materials.

2. Experimental

2.1. Dissolutions and syntheses

Reagents were purchased from Sigma-Aldrich and were used as received without further purification. The battery wastes are provided by an industrial and were used without pretreatment and contain carbon, plastics, organics and metals. The average composition in weight percentage for the major elements is the following: Cu (18–25%), Al (10–15%), Mn (14–17%), Ni (2.5–3.5%), Co (0.6–1%), Li (1.5–2%), F (0.5–2%) and P (0.2 to 0.5 %). **Dissolutions:** 15 g of wastes were dissolved in a 150 mL acidic solution under stirring. Acidic solutions were prepared with HCl (37 %):H_2O (1:1 in volume), HNO_3 (67 %):H_2O (1:3.5 in volume) or $H_2SO_4/H_2O_2/H_2O$ (1:0.3:5 in volume) mixtures. For the precipitations, different protocols have been used and will be described when needed. **Temperature study**: 1 mL of the dissolution solution was added to 1 mL of DMF containing 20 mg of BenzeneTriCarboxylic Acid (BTC). The mixture was then heated during 24 h at different temperatures (range from 20 °C to 100 °C). **Ligand ratio study:** 1 mL of the dissolution solution was added to 1 mL of DMF containing 10–40 mg of BTC and was heated during 24 h at 90 °C. For all samples, the mixture was centrifuged and the precipitate was washed 3 times with DMF, 3 times with EtOH and finally dried at 80 °C.

Digestion of the material for ICP OES analyses: 10 mg of MOF material were dissolved in a mixture of 1 mL of H_2SO_4:H_2O_2 (3:1 in volume) until the liquid was fully limpid prior analysis.

2.2. Characterizations

Materials were characterized by powder x-ray diffraction (XRD), thermogravimetric analysis (TGA), scanning electron microscopy (SEM), gas adsorption measurements, ICP OES (after digestion), and single-crystal XRD. PXRD patterns were obtained with a Bruker D8 Advance diffractometer equipped with a Cu anode. TGA were measured in a Mettler-Toledo TG with auto-sampler. A FEI Quanta 200 environmental scanning electron microscope, equipped with an Everhart-Thornley detector (ETD) and a backscattered electron detector (BSED), was used to record images with an acceleration voltage of 30 kV under high vacuum conditions. Nitrogen physisorption measurements were performed using an ASAP 2020 at 77 K, after outgassing at 363 K during 12 h, reaching a pressure below 1 mmHg, and specific surface areas were calculated using the BET method (Brunauer et al., 1938). Concentrations of metals in dissolution solutions and in materials were determined by ICP-OES analyses (Spectro ARCOS). The device was calibrated with certified standard solutions (SCP Science) and all samples were diluted in 2% HNO_3 within the range of $0-20$ ppm to meet the analysis requirements. Crystal data were collected with a Bruker APEX II diffractometer at 150 K, the absorption corrections were carried out with SADABS. The determination of the structure and the final refinement was carried out with the use of the SHELXL 2016 package.

3. Results and discussion

3.1. Dissolutions

Dissolutions of batteries (Fig. 1-A), without pretreatment, have been performed during 24 h in three different acids: hydrochloric acid, nitric acid or a mixture of sulfuric acid and H_2O_2. After dissolution, the plastics stay on the top whereas carbon material is localized at the bottom of the flask; metals are dissolved in solution (light blue color for nitric acid and green color for hydrochloric acid) (Fig. 1-B). Due to the heterogeneity of the LiB wastes, dissolution experiments have been duplicated in the same conditions and the average concentration of each metal in solutions is given by ICP OES (Fig. 1-C and Table S1). The solution with H_2SO_4/H_2O_2 will not be more discussed because it has not been possible to do metal precipitation in our conditions with this solution. We observe the total dissolution of Co, Ni, Mn and Li if we refer to the battery specifications provided by the industrial. Only the concentration of Mn in HNO_3 is lower than the one observed after dissolution in HCl, probably due to the formation Mn oxides in this acid (higher oxidizing agent). Connectors, composed of Cu and Al, have not been totally dissolved in our conditions and their concentrations in solution are more than 50 % below of the expectation. These results are coherent with a dissolution process previously reported in the literature (Billy et al., 2018), where Cu and Al have shown to act as catalysts for the total dissolution of the other metals. Finally, in these conditions, HCl shows better performances than HNO_3 for the dissolution of LiBs.

3.2. Effect of the temperature

The dissolution solutions (in HCl or HNO_3) were then mixed with a solution of DMF (ratio 1:1) containing the organic ligand (experiments are set up on 20 mg scale). The use of DMF has revealed to be crucial to solubilize the organic ligand in the final Acid/DMF mixture. After a heat treatment between 20 and 100 °C for 24 h, precipitates are observed for some temperatures. Materials are then isolated by centrifugation and washed thoroughly with DMF and EtOH, and finally dried in an oven (40 °C). No precipitate was observed below 70 °C. Between 70 and 100 °C, white powders were observed at the bottom of the flask. After digestion of the materials, the metal composition of the precipitates was determined by ICP-OES (Fig. 2-A). Results reveal that materials are composed in majority of Al for all temperatures and whatever the acid used for the dissolution of the battery. By increasing the temperature from 70 °C to 100 °C, it was observed a larger amount of precipitate but also an increase of the quantity of impurities, up to around 15 % of other metals that co-precipitate with Al-MOFs at 100 °C. PXRD patterns of the different powders appear remarkably similar and indicate a highly crystalline structure for these materials (Fig. 2-B and -C). Matching peaks with a reported structure (Loiseau et al., 2006) indicates the formation of the MIL-96(Al) MOF in the battery waste solution. The formation of the MIL-96 phase, compared to other structures composed of Al and BTC (e.g. MIL-110 or MIL-100 phases), is coherent with the presence of acids during the formation of the materials in our conditions. MIL-110 and MIL-100 phases can be synthesized in very highly acidic conditions (pH 0-0.3 for MIL-110 and pH 0.5-0.7 for MIL-100), whereas the MIL-96 phase can only be formed at pH values between 1 and 3 (Volkringer et al., 2009).

Finally, the amount of MOF obtained is optimal at 90 °C, and further analyses will be performed at this optimized temperature.

Materials were activated to fully remove impurities and solvents from the cavities prior analyses. TGA analyses are in accordance with a material composed as : $Al_{12}O(OH)_{18}(H_2O)_5[BTC]_6 \sim 29H_2O$ corresponding to MIL-96 (Loiseau et al., 2006) (Fig. 3-A). The loss of water molecules was observed until 200 °C (18 % weight loss) and DMF molecules until 350 °C (11 % weight loss) prior the degradation of the framework at 400 °C with the loss of the organic ligand (44 % weight loss) to form Al_2O_3 as inorganic residue (25 % (HCl) and 28 % (HNO_3)). Nitrogen uptake experiments have revealed similar specific surface area to that reported in the literature(623 $m^2.g^{-1}$ (HCl) and 718 $m^2.g^{-1}$ (HNO_3)), underlining the purity of the materials (Maes et al., 2010) (Fig. 3-B). Finally, SEM images have revealed homogeneous particles with rice grain shape of length around 400 nm (in HNO_3) and 300 nm (in HCl) (Fig. 3-C-D). Probably due to the smaller particle size of materials obtained in HCl some significant agglomeration was observed.

3.3. Ligand ratio

The quantity of ligands necessary for the precipitation has also been studied. In our conditions, the quantity of ligand has been tested from 10–40 mg with a volume of battery waste of 1 ml. In all conditions, a precipitate was observed and materials exhibit a white color, except for 30 mg and 40 mg of ligand in HNO_3 where some blue crystals mixed to the white powder can be observed and suggest the presence of different MOFs.

Metal compositions of the materials have been determined by ICP-OES after digestion of the different materials (Fig. 4-A). All materials are composed in majority of Al as expected. In the case of a metal precipitation in presence of HCl, the quantity of Ni and Mn inside the material increases with an increase of ligand, but PXRD patterns of the materials are identical to the MIL-96 pattern (Fig. SI-2). While using HNO_3 acid during the synthesis and 10–25 mg of ligand, metals inside the MOFs are composed of Al for more than 90 %. Finally, with 30–40 mg of ligand, color of the powders change from white to blue corresponding to a higher Cu precipitation inside the resulting powder (Fig. 4-B). PXRD patterns reveal new pics (Fig. SI-2) and the structure of the blue crystals has been solved by single crystal XRD analysis. It reveals the co-precipitation of a Cu based MOF with a HKUST-1 structure in addition to the MIL-96 (Fig. 4-C).

Finally, optimal parameters to obtain materials with the higher purity are the use of 20 mg of ligands (Fig. SI-3) and a heat treatment of 90 °C in our conditions. These parameters allow to totally remove Al from the dissolution solution with low co-precipitation of other materials, and will be used in the next part of this work.

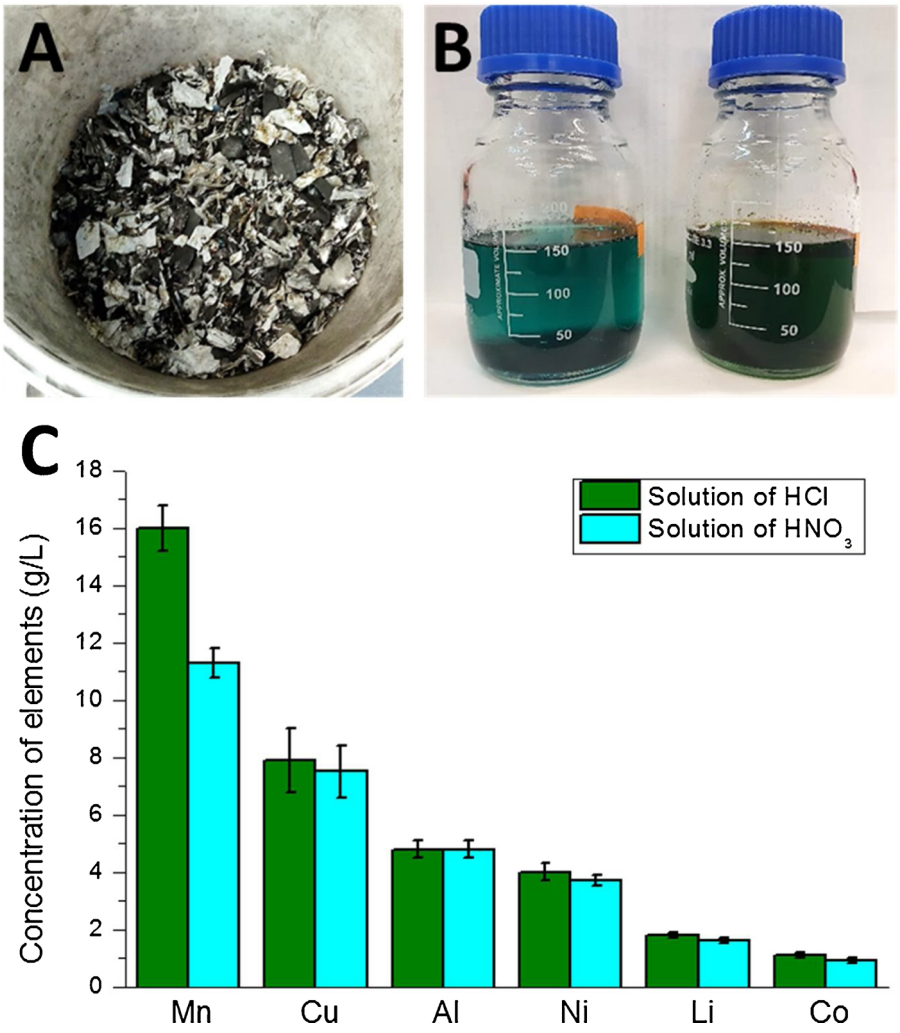

Fig. 1. (A) LMN battery wastes, (B) Dissolution of battery wastes in HCl (left) and HNO_3 (right), (C) Metal composition of the battery waste dissolution solutions (ICP-OES).

3.4. Multi step precipitations

After precipitation of the first MOF and precipitation of the Al, the supernatant is recovered and a new batch of BTC ligand (20 mg) was introduced to the solution. The mixture was then heated again for another 24 h to try to isolate other metals in MOFs materials. After this second step, new precipitates indeed appeared and after analyses, the formation of two new different MOFs was confirmed, depending on the conditions of synthesis (HCl or HNO_3).

In HCl, the PXRD pattern of the material (Fig. 5-B) reveals the formation of a crystalline organic-inorganic material with no correspondence with other materials described in the literature. This material is composed of Ni and Mn in a 1:3 ratio (Fig. 5-A) and exhibits square shapes with lateral size of around 1 µm (Fig. 5-D). From TGA (Fig. 5-C), a loss of water molecules was observed from 105 °C (4 % weight loss) and DMF molecules from 180 °C (31 % weight loss) prior to the degradation of the framework at 290 °C with the loss of the organic ligand (31 % weight loss) to form a metal oxide (inorganic residue of 34%). PXRD analyze of the residue has shown the presence of $NiMn_2O_4$ (Fig. SI-4). Starting from $NiMn_2BTC_2.4DMF \sim 2\ H_2O$ formula a theoretical weigh loss of 4% of water, 32% of DMF and 38% of organic moiety to form an inorganic residue of $NiMn_2O_4$ (26%) should be observed. TGA profile was not in accordance with this theoretical analyze due to the presence of amorphous impurities composed of Manganese. Taking into account the ICP-OES analysis of the material after digestion metal ratio of the MOF should be Mn/Ni (3:1). It is supposed the presence of free Mn ($MnCl_2$ or MnO_2) sorbed inside the MOF cavity that is converted after a heat treatment under air to Mn_3O_4. TGA profile is then in accordance with a loss 4% of water (4 % obs.), 28 % of DMF (31 % obs.) and the degradation of 36 % (31% obs.) of organic moieties from $\mathbf{NiMn_2BTC{\cdot}4DMF \sim 2\ H_2O{\cdot}MnCl_2}$ to form 32 % (34% obs.) of $NiMn_2O_4$ and amorphous Mn_3O_4 at 1000 °C.

In HNO_3, it is observed the formation of a material, whose PXRD pattern (Fig. 5-B) matches that of HKUST-1 (as observed during the ligand ratio experiments discussed above) and a metal composition of Cu-Mn (4:6) (Fig. 5-A). SEM image reveals that the material is composed of small crystals (around 5 µm) with polygon shapes (Fig. 5-D). TGA analysis (Fig. 5**-C**) exhibits a loss of water molecules was observed until 160 °C (12 % weight loss) and DMF molecules until 210 °C (12% weight loss) prior the degradation of the framework in two steps at 250 °C, with an organic weight loss of 29 %, and 297 °C with a weight loss of 15%. The inorganic residue represented 32% of the weight and formed of CuO and (Cu-Ni-Mn) hybrid oxide according to the PXRD analysis of the residue (Fig. SI-5). To match to the ICP-OES analyses (1 Ni for 4 Cu and 6 Mn), it is proposed the formation of two different MOFs and, as explained previously, the presence of Manganese, salts or

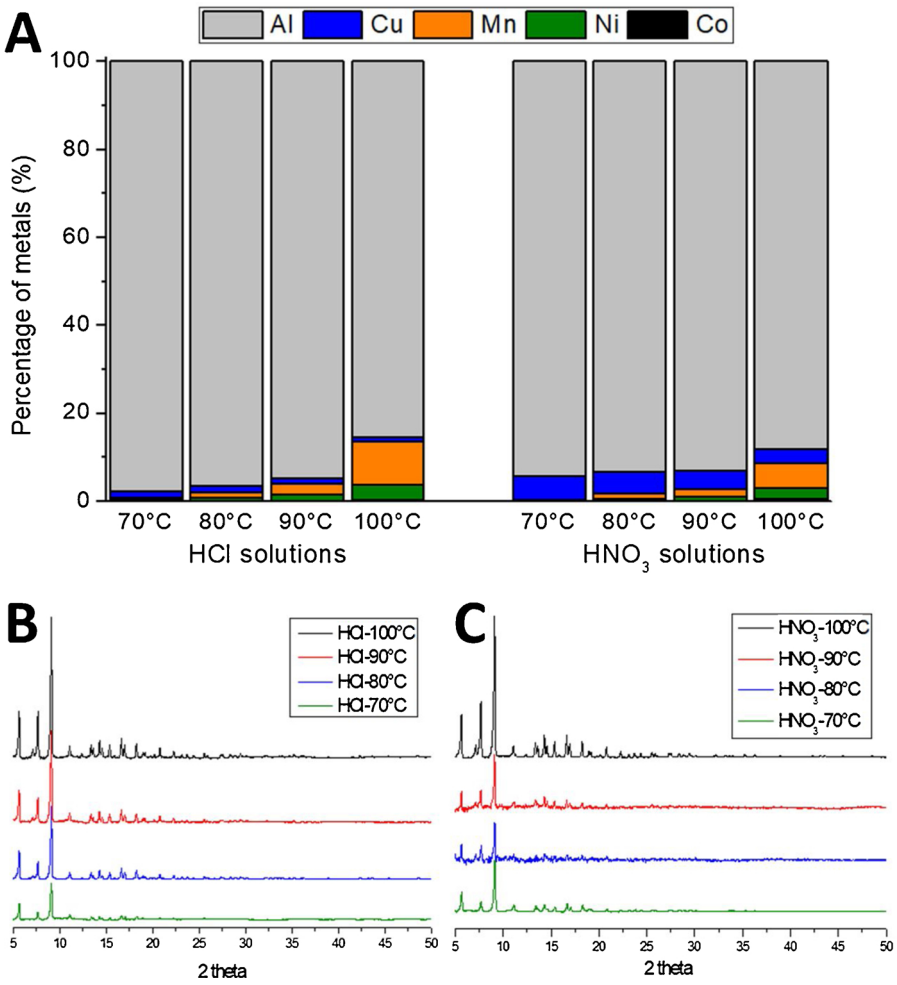

Fig. 2. (A) Metal composition of the precipitates obtained at different temperatures in HNO_3 and in HCl. PXRD patterns of materials in HCl (B) and HNO_3 (C).

oxide, trapped inside the MOF. Starting from **$NiMn_2BTC_2{\cdot}4/3(Cu_3BTC_2){\cdot}4(Mn(NO_3)_2{\cdot}H_2O){\cdot}4DMF \sim 19H_2O$** it is supposed a loss of 12 % of water (12 % obs.), 11 % of DMF (12 % obs.) followed by the degradation of the mixed Cu-MOF and the Mn impurities to form CuO and MnO_2 with 32 % weight loss (29 % obs.) and finally the degradation of the Ni/Mn-MOF with a loss of 13 % (15 % obs.). The final inorganic residues (32 %, 32 % obs.) are a mixture of CuO and a hybrid (Cu-Ni-Mn) oxides ($[Cu(Mn_{0.748}Ni_{0.252})_2O_4]$, $[Cu_{0.8}Ni_{0.2}Mn_2O_4]$).

After reaction and centrifugation of the materials, the supernatant is then used again for a third addition of BTC ligand (20 mg) in a third step. In this case, a very small amount of materials is recovered (around 10 % of what has been recovered for the second step). Moreover, these materials have revealed the same compositions and structures, in both cases (Figs. 5A and SI-6). This experiment has shown that in this condition, it is no more possible to precipitate other metals.

Finally the scale-up of the reaction (by a factor 100) has been performed by increasing the quantity of ligand (2 g) and the volume of the dissolution solution (100 ml). Same protocols than previously described were used, and the process was stopped after step two. The three different materials obtained have been analyzed, and no difference can be found between these materials and those obtained in smaller scale syntheses. With 2 g of BTC and 100 mL of dissolution solution, 4.5 g of MIL-96 is synthetized. Then adding 2 more g of BTC, 5 g of Ni-Mn-MOF or Cu-MOF are obtained depending of the acidic condition.

These quantitative results for the recycling of batteries as MOFs are very encouraging in the perspective of scaling up this process according to the flow scheme depicted in Fig. 6.

3.5. Economic benefit analysis

Today very few amount of LiBs are recycled because their recycling processes are very complex with low economic benefits due to the low price of recovered metals (e.g. 1 kg of Co cost around 30 USD in 2019). Here we propose a proof of concept to generate high valuable materials from spent LiBs. The requirement of energy is less to produce value-added products compare to pyrometallurgical method which involves very high temperature.

In **Table S7**, laboratory-scale economic assessments show the cost to obtain 1 kg of MIL-96 from 3 kg of spent LiBs (first step of this recycling process). It reveals than almost half of the cost is due to the use of DMF and that for 1 kg of MIL-96, obtained in the first recycling step, we need between 1300 to 1400 USD of chemicals and an extra 220 USD to obtain 1 more kg of HKUST-1, in a second precipitation step. MIL-96 is not available on the market because no company is able to synthesis this material at large scale. Anyway the price for 1 kg of MIL-53 (obtained with BenzeneDiCarboxylic acid as ligand and Al) is 11,080 USD and HKUST-1 (MOF obtained in the second precipitation step in HNO_3) is 21,900 USD in 2019. The protocol is not environmental friendly due to the high quantity of acid and organic solvent used but it can be optimized to decrease the cost of the valuable products and to be suitable

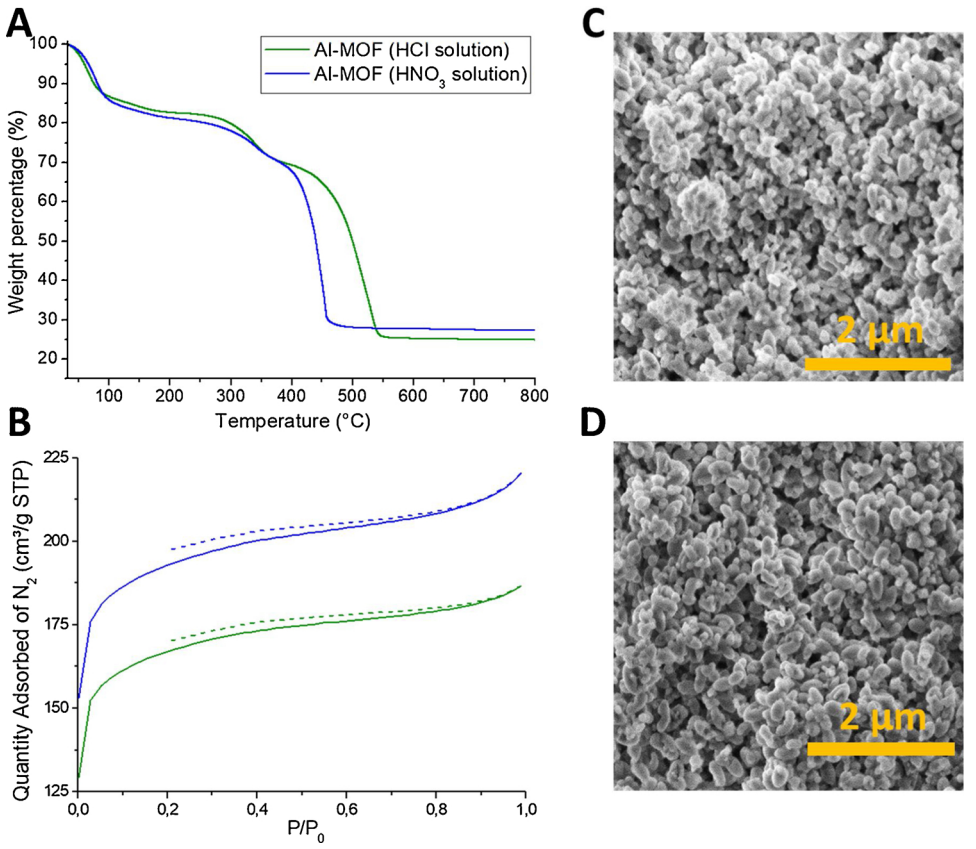

Fig. 3. (A) TGA analyses of Al-MOFs, (B) Nitrogen uptake measurements of Al-MOFs (adsorption in solid line and desorption in dash line), (C) and (D) SEM images of Al-MOF(HCl) and Al-MOF(HNO_3), respectively.

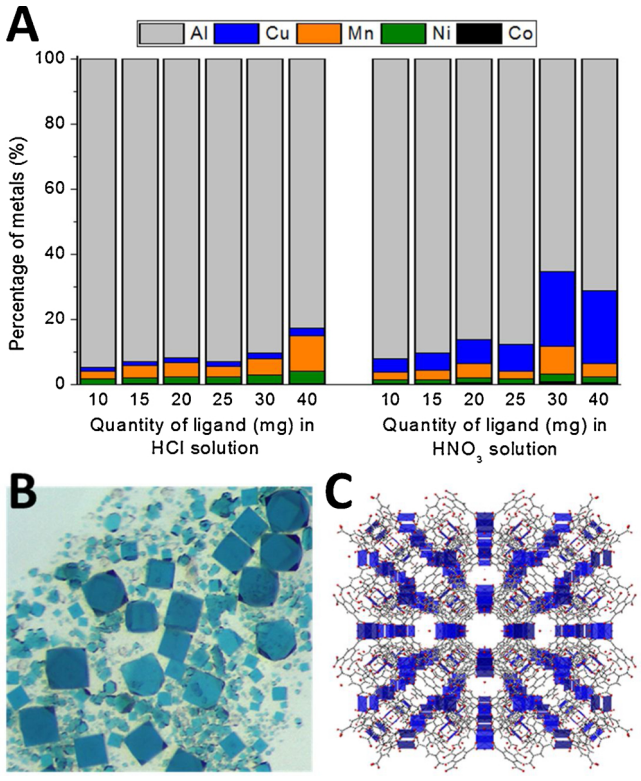

Fig. 4. (A) Metal composition of materials obtained with different quantity of ligand, (B) photograph of a precipitate from a mixture involving 30 mg of ligands in HNO_3 and (C) structure of the HKUST-1 material.

with the industry. Moreover residual wastes of this process can then be treated to recover other metals that have not precipitate to add some value to the recycling process.

Finally, it is difficult to compare this method with others as the strategy is totally different but as MOFs are expensive materials and that only a low number of them can be synthesis in large amount, we believe that it can be considered to form such materials with wastes to make wastes valuable. Life cycle analysis including such process can be envisaged after the optimization of the process.

4. Conclusion

An original strategy is proposed for the recycling of Li-Ion batteries with the production of valuable materials from wastes. Under specific conditions, it has been possible to produce Al-MOFs with high purity and porosity able to remove all the Al from a battery waste dissolution solution by specific metal precipitation. In a second step, after the removal of Al, two other materials can be recovered, containing high quantity of Ni/Mn or Cu/Ni/Mn metals depending on the involved acid. Both materials present high quality but co-precipitation of Manganese can be observed. Where Al and Cu-MOFs are already known for their interesting gas storage capacity (MIL-96 and HKUST-1, respectively), the other Ni/Mn-MOF can potentially have some interest as new electrode material and close the loop of a battery recycling process.

Here is presented a proof of concept that has to be optimized to follow the industrial requirements. Moreover, this process should be tested with other battery waste sources containing different metal ratios or with pre-treated wastes, where connectors (Al, Cu) have already been separated. Finally, the production of valuable materials as MOFs, potentially in large scale, from wastes seems to be an interesting possibility to solve the production of MOFs and to reduce the volume of battery waste.

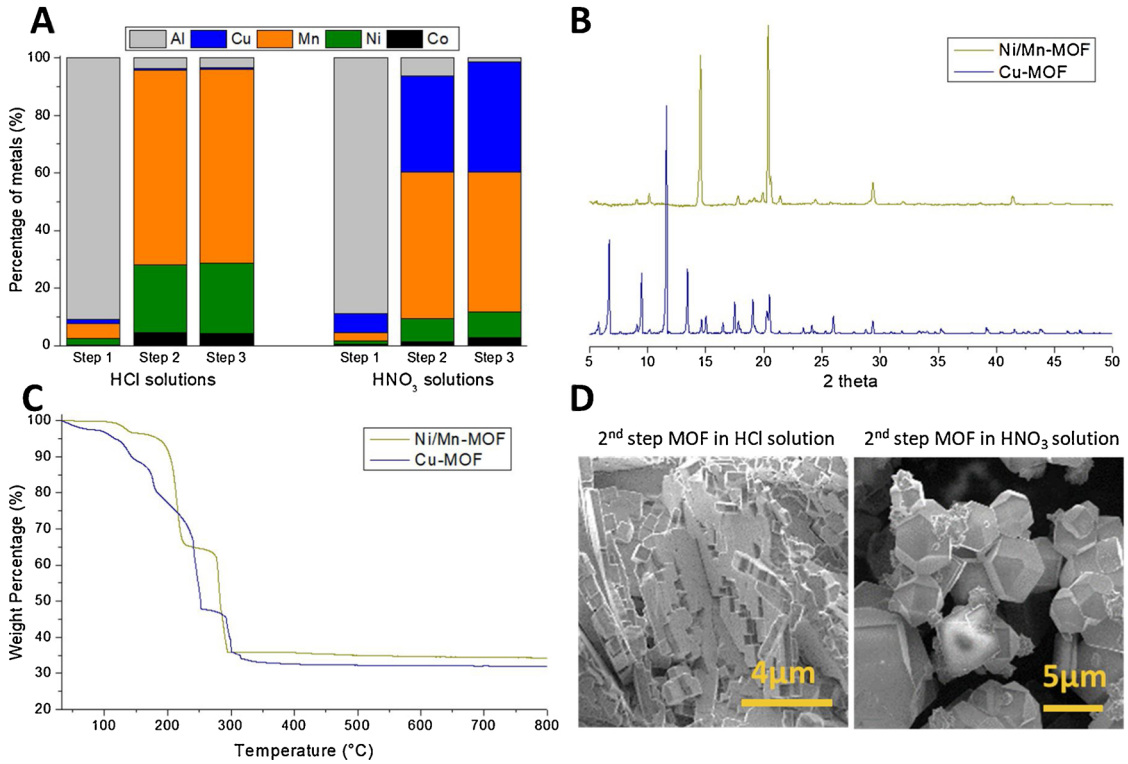

Fig. 5. (A) Metal composition of materials obtained at different steps of precipitation (see text for details), (B) PXRD, (C) TGA and (D) SEM images of Ni/Mn-MOF and Cu-MOF obtained after multi-step precipitation.

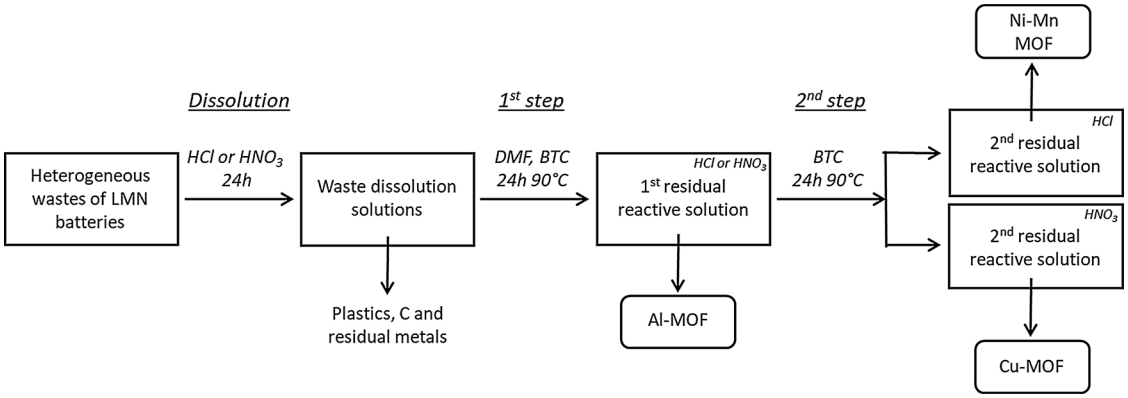

Fig. 6. Flow chart of the recycling method of Li-ion batteries.

Acknowledgments

Authors are grateful to Joseph Lautru and Xavier Le Goff for their respective help for SEM analyses and single crystal XRD and to the CEA and NTU for supporting this research through the SCARCE project.

Appendix A. Supplementary data

Supplementary material related to this article can be found, in the online version, at doi:https://doi.org/10.1016/j.jhazmat.2019.121603.

References

Whittingham, M.S., 2012. History, evolution, and future status of energy storage. Proc. IEEE 100, 1518–1534. https://doi.org/10.1109/JPROC.2012.2190170.
Tarascon, J.-M., Armand, M., 2001. Issues and challenges facing rechargeable lithium batteries. Nature 414, 359–367. https://doi.org/10.1038/35104644.
Rozier, P., Tarascon, J.M., 2015. Review—Li-Rich layered oxide cathodes for next-generation Li-Ion batteries: chances and challenges. J. Electrochem. Soc. 162, A2490–A2499. https://doi.org/10.1149/2.0111514jes.
Dimesso, L., Förster, C., Jaegermann, W., Khanderi, J.P., Tempel, H., Popp, A., Engstler, J., Schneider, J.J., Sarapulova, A., Mikhailova, D., Schmitt, L.A., Oswald, S., Ehrenberg, H., 2012. Developments in nanostructured LiMPO4 (M = Fe, Co, Ni, Mn) composites based on three dimensional carbon architecture. Chem. Soc. Rev. 41, 5068. https://doi.org/10.1039/c2cs15320c.
Pillot, C., 2017. The Rechargeable Battery Market and Main Trends 2016–2025.
Cheng, E.J., Hong, K., Taylor, N.J., Choe, H., Wolfenstine, J., Sakamoto, J., 2017. Mechanical and physical properties of LiNi 0.33 Mn 0.33 Co 0.33 O 2 (NMC). J. Eur. Ceram. Soc. 37, 3213–3217. https://doi.org/10.1016/j.jeurceramsoc.2017.03.048.
Susai, F.A., Sclar, H., Shilina, Y., Penki, T.R., Raman, R., Maddukuri, S., Maiti, S., Halalay, I.C., Luski, S., Markovsky, B., Aurbach, D., 2018. Horizons for Li-ion batteries relevant to electro-mobility: high-specific-energy cathodes and chemically active separators. Adv. Mater. 30, 1801348. https://doi.org/10.1002/adma.201801348.
Jacoby, M., 2019. It's time to get serious about recycling lithium-ion batteries. Chem. Eng. News 97.
Ciez, R.E., Whitacre, J.F., 2019. Examining different recycling processes for lithium-ion batteries. Nat. Sustain. 2, 148–156. https://doi.org/10.1038/s41893-019-0222-5.
Anon, 2019. Recycle spent batteries. Nat. Energy 4, 253. https://doi.org/10.1038/s41560-019-0376-4.
Liu, K., Tan, Q., Liu, L., Li, J., 2019. Acid-free and selective extraction of lithium from spent lithium iron phosphate batteries via a mechanochemically induced isomorphic substitution. Environ. Sci. Technol. 53, 9781–9788. https://doi.org/10.1021/acs.est.

9b01919.
Zhang, X., Li, L., Fan, E., Xue, Q., Bian, Y., Wu, F., Chen, R., 2018. Toward sustainable and systematic recycling of spent rechargeable batteries. Chem. Soc. Rev. 47, 7239–7302. https://doi.org/10.1039/C8CS00297E.
Vikström, H., Davidsson, S., Höök, M., 2013. Lithium availability and future production outlooks. Appl. Energy 110, 252–266. https://doi.org/10.1016/j.apenergy.2013.04.005.
Anon, 2013. The urban mining concept. Waste Manag. 33, 497–498. https://doi.org/10.1016/j.wasman.2013.01.010.
Grey, C.P., Tarascon, J.M., 2017. Sustainability and in situ monitoring in battery development. Nat. Mater. 16, 45–56. https://doi.org/10.1038/nmat4777.
Xu, J., Thomas, H.R., Francis, R.W., Lum, K.R., Wang, J., Liang, B., 2008. A review of processes and technologies for the recycling of lithium-ion secondary batteries. J. Power Sources 177, 512–527. https://doi.org/10.1016/j.jpowsour.2007.11.074.
Chagnes, A., Pospiech, B., 2013. A brief review on hydrometallurgical technologies for recycling spent lithium-ion batteries: technologies for recycling spent lithium-ion batteries, J. Chem. Technol. Biotechnol. 88, 1191–1199. https://doi.org/10.1002/jctb.4053.
Barik, S.P., Prabaharan, G., Kumar, B., 2016. An innovative approach to recover the metal values from spent lithium-ion batteries. Waste Manag. 51, 222–226. https://doi.org/10.1016/j.wasman.2015.11.004.
Gao, W., Zhang, X., Zheng, X., Lin, X., Cao, H., Zhang, Y., Sun, Z., 2017. Lithium carbonate recovery from cathode scrap of spent lithium-ion battery: a closed-loop process. Environ. Sci. Technol. 51, 1662–1669. https://doi.org/10.1021/acs.est.6b03320.
Rothermel, S., Evertz, M., Kasnatscheew, J., Qi, X., Grützke, M., Winter, M., Nowak, S., 2016. Graphite recycling from spent lithium-ion batteries. ChemSusChem 9, 3473–3484. https://doi.org/10.1002/cssc.201601062.
Cui, Y., Li, B., He, H., Zhou, W., Chen, B., Qian, G., 2016. Metal–organic frameworks as platforms for functional materials. Acc. Chem. Res. 49, 483–493. https://doi.org/10.1021/acs.accounts.5b00530.
Li, J.-R., Kuppler, R.J., Zhou, H.-C., 2009. Selective gas adsorption and separation in metal-organic frameworks. Chem. Soc. Rev. 38, 1477. https://doi.org/10.1039/b802426j.
Cognet, M., Gutel, T., Peralta, D., Maynadié, J., Carboni, M., Meyer, D., 2017. Communication—iron(II)-benzene phosphonate coordination polymers as an efficient active material for negative electrode of lithium-ion batteries. J. Electrochem. Soc. 164, A2552–A2554. https://doi.org/10.1149/2.1231712jes.
Silva, P., Vilela, S.M.F., Tomé, J.P.C., Almeida Paz, F.A., 2015. Multifunctional metal–organic frameworks: from academia to industrial applications. Chem. Soc. Rev. 44, 6774–6803. https://doi.org/10.1039/C5CS00307E.
Muller, U., Schubert, M., Teich, F., Puetter, H., Schierle-Arndt, K., Pastré, J., 2006. Metal–organic frameworks—prospective industrial applications. J. Mater. Chem. 16, 626–636. https://doi.org/10.1039/B511962F.
Yilmaz, B., Trukhan, N., Müller, U., 2012. Industrial outlook on zeolites and metal organic frameworks. Chin. J. Catal. 33, 3–10. https://doi.org/10.1016/S1872-2067(10)60302-6.
Chui, S.S., 1999. A chemically functionalizable nanoporous material [Cu3(TMA)2(H2O)3]n. Science 283, 1148–1150. https://doi.org/10.1126/science.283.5405.1148.
U. Muller, H. Puetter, M. Hesse, H. Wessel, WO 2005/049892, n.d.
Peng, Y., Krungleviciute, V., Eryazici, I., Hupp, J.T., Farha, O.K., Yildirim, T., 2013. Methane storage in metal–organic frameworks: current records, surprise findings, and challenges. J. Am. Chem. Soc. 135, 11887–11894. https://doi.org/10.1021/ja4045289.
Xiao, B., Wheatley, P.S., Zhao, X., Fletcher, A.J., Fox, S., Rossi, A.G., Megson, I.L., Bordiga, S., Regli, L., Thomas, K.M., Morris, R.E., 2007. High-capacity hydrogen and nitric oxide adsorption and storage in a metal − organic framework. J. Am. Chem. Soc. 129, 1203–1209. https://doi.org/10.1021/ja066098k.
Liu, J., Wang, Y., Benin, A.I., Jakubczak, P., Willis, R.R., LeVan, M.D., 2010. CO_2 /H_2O adsorption equilibrium and rates on metal − organic frameworks: HKUST-1 and Ni/DOBDC. Langmuir 26, 14301–14307. https://doi.org/10.1021/la102359q.
James, S.L., Adams, C.J., Bolm, C., Braga, D., Collier, P., Friščić, T., Grepioni, F., Harris, K.D.M., Hyett, G., Jones, W., Krebs, A., Mack, J., Maini, L., Orpen, A.G., Parkin, I.P., Shearouse, W.C., Steed, J.W., Waddell, D.C., 2012. Mechanochemistry: opportunities for new and cleaner synthesis. Chem. Soc. Rev. 41, 413–447. https://doi.org/10.1039/C1CS15171A.
Ali-Moussa, H., Navarro Amador, R., Martinez, J., Lamaty, F., Carboni, M., Bantreil, X., 2017. Synthesis and post-synthetic modification of UiO-67 type metal-organic frameworks by mechanochemistry. Mater. Lett. 197, 171–174. https://doi.org/10.1016/j.matlet.2017.03.140.
Brunauer, S., Emmett, P.H., Teller, E., 1938. Adsorption of Gases in Multimolecular Layers. J. Am. Chem. Soc. 60, 309–319. https://doi.org/10.1021/ja01269a023.
Billy, E., Joulié, M., Laucournet, R., Boulineau, A., De Vito, E., Meyer, D., 2018. Dissolution mechanisms of $LiNi_{1/3}Mn_{1/3}Co_{1/3}O_2$ positive electrode material from lithium-ion batteries in acid solution. ACS Appl. Mater. Interfaces 10, 16424–16435. https://doi.org/10.1021/acsami.8b01352.
Loiseau, T., Lecroq, L., Volkringer, C., Marrot, J., Férey, G., Haouas, M., Taulelle, F., Bourrelly, S., Llewellyn, P.L., Latroche, M., 2006. MIL-96, a porous aluminum trimesate 3D structure constructed from a hexagonal network of 18-membered rings and μ_3-oxo-centered trinuclear units. J. Am. Chem. Soc. 128, 10223–10230. https://doi.org/10.1021/ja0621086.
Volkringer, C., Popov, D., Loiseau, T., Férey, G., Burghammer, M., Riekel, C., Haouas, M., Taulelle, F., 2009. Synthesis, single-crystal X-ray microdiffraction, and NMR characterizations of the giant pore metal-organic framework aluminum trimesate MIL-100. Chem. Mater. 21, 5695–5697. https://doi.org/10.1021/cm901983a.
Maes, M., Alaerts, L., Vermoortele, F., Ameloot, R., Couck, S., Finsy, V., Denayer, J.F.M., De Vos, D.E., 2010. Separation of C_5-Hydrocarbons on microporous materials: complementary performance of MOFs and zeolites. J. Am. Chem. Soc. 132, 2284–2292. https://doi.org/10.1021/ja9088378.